8

BASIC PRINCIPLES OF ATMOSPHERIC SENSING AND RADIATIVE TRANSFER

The interactions of electromagnetic waves with planetary atmospheres are governed by the characteristics of the propagating wave (mainly its wavelength), the physical characteristics of the atmosphere (pressure, temperature, and suspended particulates), and its constituents. These interaction mechanisms are relatively complex to model because of the three-dimensional nature of the propagation medium and the multiplicity of the interaction mechanisms: scattering, absorption, emission, and refraction.

In this chapter, we give a brief overview of the physical and chemical properties of planetary atmospheres that are relevant to remote sensing. The basic concepts of temperature, composition, pressure, density, and wind sensing will be established as an introduction to the more detailed analysis in the following chapters.

8-1 PHYSICAL PROPERTIES OF THE ATMOSPHERE

The atmospheric density decreases with altitude. In the case of hydrostatic equilibrium, the pressure $p(z)$ and density $\rho(z)$ are related by the following relationship:

$$dp(z) = -g\rho(z)dz \tag{8-1}$$

where g is the planet's gravity, assumed to be constant through the thin atmospheric layer, and p is measured vertically upward from the surface. The above expression basically states that the difference of pressure between levels z and $z + dz$ is equal to the weight of the atmosphere between these two levels.

Introduction to the Physics and Techniques of Remote Sensing. By C. Elachi and J. van Zyl

The equation of state for a perfect gas relates the pressure and density by

$$\rho(z) = MM_0 \frac{p(z)}{kT(z)}$$

or

$$N(z) = \frac{p(z)}{kT(z)} \tag{8-2}$$

where M is the average molecular weight of the atmosphere ($M = 28.97$ for the Earth's atmosphere), M_0 is the atomic mass unit ($M_0 = 1.66 \times 10^{-27}$ kg), k is Boltzmann's constant ($k = 1.38 \times 10^{-23}$ JK^{-1}), N is the number density (molecules/m^3), and T is the temperature. Combining Equations 8-1 and 8-2 we get

$$\frac{dp}{p} = -g\frac{MM_0}{kT(z)}dz = -\frac{dz}{H(z)} \tag{8-3}$$

where

$$H(z) = \frac{kT(z)}{gMM_0} \tag{8-4}$$

H is known as the scale height. The solution for Equation 8-3 is simply

$$p(z) = p(0)\exp\left[-\int_0^z \frac{d\zeta}{H(\zeta)}\right] \tag{8-5}$$

where $p(0)$ is the surface pressure. In the case of an isothermal atmosphere (T = constant),

$$p(z) = p(0)\exp\frac{-z}{H} \tag{8-6}$$

which shows that the pressure decreases exponentially with altitude. The same is true for the density

$$\rho(z) = \rho(0)\exp\frac{-z}{H} \tag{8-7}$$

where

$$\rho(z) = \frac{MM_0 p(0)}{kT} = \frac{p(0)}{gH} \tag{8-8}$$

Similarly, the number density N (molecules/m^3) is given by

$$N(z) = N(0)\exp\frac{-z}{H} \tag{8-9}$$

By integrating Equation 8-7, we get the total atmospheric mass M_T in a column of unit area:

$$M_T = \int_0^\infty \rho(z)dz = \rho(0)H = \frac{p(0)}{g} \tag{8-10}$$

This shows that the scale height corresponds to the thickness of a homogeneous atmospheric layer of density $\rho(0)$ and mass equal to the atmospheric mass.

To illustrate, in the case of the Earth's atmosphere, we have $M = 28.97$, $p(0) = 1$ atmosphere $= 10^5$ Newton/m^2, $g = 9.81$ m/sec^2, and $T = 288$ K. This gives:

$H = 8.4$ km (from Equation 8-4)

$\rho(0) = 1.21$ kg/m^3 (from Equation 8-8)

$M_T = 10.200$ kg/m^2 (from Equation 8-10)

Table 8-1 gives some of the parameters for the atmosphere of Venus, Mars, and Titan.

Most of the atmospheric mass is in a very thin layer above the surface relative to the planet's radius. In the case of the Earth, 99% of the atmospheric mass is below 32 km. Thus, in most models, the atmosphere is considered as a locally plane parallel slab, and the planetary curvature is neglected except in the case of limb sounding and occultation experiments.

The above illustrations assumed an isothermal atmosphere. Usually, this is not exactly true. In the case of the Earth, the temperature near the surface decreases as a function of altitude up to an altitude of 11 km, then remains constant up to the 25 km level. The change of the atmospheric temperature can be derived for a simplified case in which it is assumed that the atmosphere is transparent to all radiation and contains no liquid particles. If we assume a unit mass moving upward in an atmosphere in hydrostatic equilibrium, the first law of thermodynamics gives

$$C_v dT + p\, dV = dq = 0 \tag{8-11}$$

where C_v is the specific heat at constant volume, dV is the change in volume, dT is the change in temperature, and dq is the heat input, which is equal to zero. Differentiating the equation of state (Equation 8-2) and remembering that $\rho = 1/V$, we get

$$p\, dV + V\, dp = \frac{k}{MM_0} dT \tag{8-12}$$

TABLE 8-1. Some Properties of Planetary Atmospheres

	Venus	Earth	Mars	Titan
Surface pressure (bar)	90	1	0.02	1-3
Surface temperature (K)	880	290	~250	~94
Scale height (km)	15	8.4	~10	~20
Main constituents	97% CO_2	78% N_2	CO_2	CH_4
	N_2	21% O_2	N_2	
		1% Ar	Ar	
		H_2O, CO_2, O_3		

For a perfect gas we have $k/MM_0 = C_p - C_v$, where C_p is the specific heat at constant pressure. Combining Equations 8-11 and 8-12 we get:

$$V\,dp = C_p dT$$

Replacing dp by its value from Equation 8-1, we get

$$\frac{dT}{dz} = -\frac{g}{C_p} = -\Gamma_a \tag{8-13}$$

where Γ_a is known as the adiabatic lapse rate. For the Earth's atmosphere, $C_p \simeq 1000$ J/kg K. This gives

$$\Gamma_a = 9.81 \text{ K/km}$$

If the temperature at the bottom of the atmosphere is equal to $T(0)$, then the solution for Equation 8-12 gives the temperature profile as

$$T(z) = T(0) - \Gamma_a z \tag{8-14}$$

In reality, the temperature in the Earth's lower atmosphere does decrease linearly with altitude but at a rate of 6.5 K/km, somewhat lower than Γ_a. At higher altitudes, the temperature profile is significantly more complex, as shown in Figure 8-1.

8-2 ATMOSPHERIC COMPOSITION

The composition of the atmosphere varies significantly among planets, as shown in Table 8-1. In the case of the Earth, carbon dioxide, water vapor, and ozone dominate the interaction with electromagnetic radiation. Carbon dioxide is substantially uniformly mixed up to about 100 km. The interaction of the CO_2 molecule with electromagnetic waves is strongest in the infrared region, near 4.3 μm and 15 μm. It plays a dominant role in the energy budget of the mesosphere (50 to 90 km), which is cooled as a result of CO_2 radiative emission in the 15 μm band.

Water vapor plays an important role in the energy budget of the troposphere (below about 15 km) because of its role in cloud formation, precipitation, and energy transfer in the form of latent heat. Water vapor concentration is highly variable in space and time. At sea level, it varies from 10^{-2} g/m^3 in a very cold, dry climate up to 30 g/m^3 in hot, humid regions. The density decreases exponentially as a function of altitude with a scale height of about 2.5 km. For an average surface density of 10 g/m^3 the total columnar mass per unit area is 25 kg/m^2, which is about 0.25% of the total atmospheric mass. However, it is particularly important in remote sensing because of the strong water vapor absorption lines in the infrared (Fig. 8-2) and microwave regions.

Ozone strongly absorbs ultraviolet radiation and causes a shortwave cutoff of the Earth's transmission at 0.3 μm and shorter. It is mostly concentrated between 20 and 50 km altitude, and its distribution is also highly variable. The formation and dissociation of ozone involves a series of complex chemical catalytic reactions among nitrogen, hydrogen, and chlorine compounds, some of which arise from human activities.

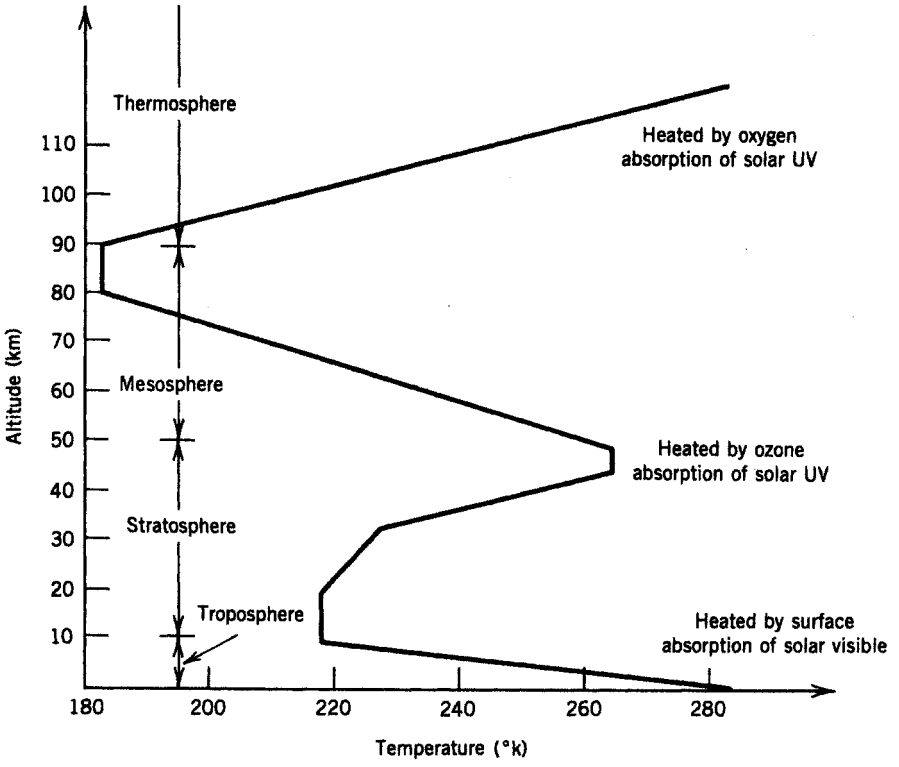

Figure 8-1. Temperature profile of the Earth's atmosphere.

In addition to CO_2, H_2O, and O_3 a number of other minor constituents play a role in the Earth's upper atmosphere chemistry. The distribution of some of these constituents is shown in Figure 8-3.

8-3 PARTICULATES AND CLOUDS

Particulates are atmospheric dust particles of radii between 0.1 and 10 μm. Clouds of liquid and solid water have particles of size varying between 1 and 100 μm. Particulates are usually concentrated in the lowest few kilometers and tend to scatter radiation in the visible and near- to mid-IR regions. Particulates can be ejected directly into the atmosphere or formed in the visible atmosphere from trace gases.

The height distribution of the number density of large particles can also be approximated by an exponential decay similar to Equation 8-9:

$$N(z) = N(0) \exp \frac{-z}{H_p} \tag{8-15}$$

where H_p is the particles' scale height. In the case of large particles in the Earth's atmosphere, H_p is about 1 km. The other important factor is the size distribution of the particles.

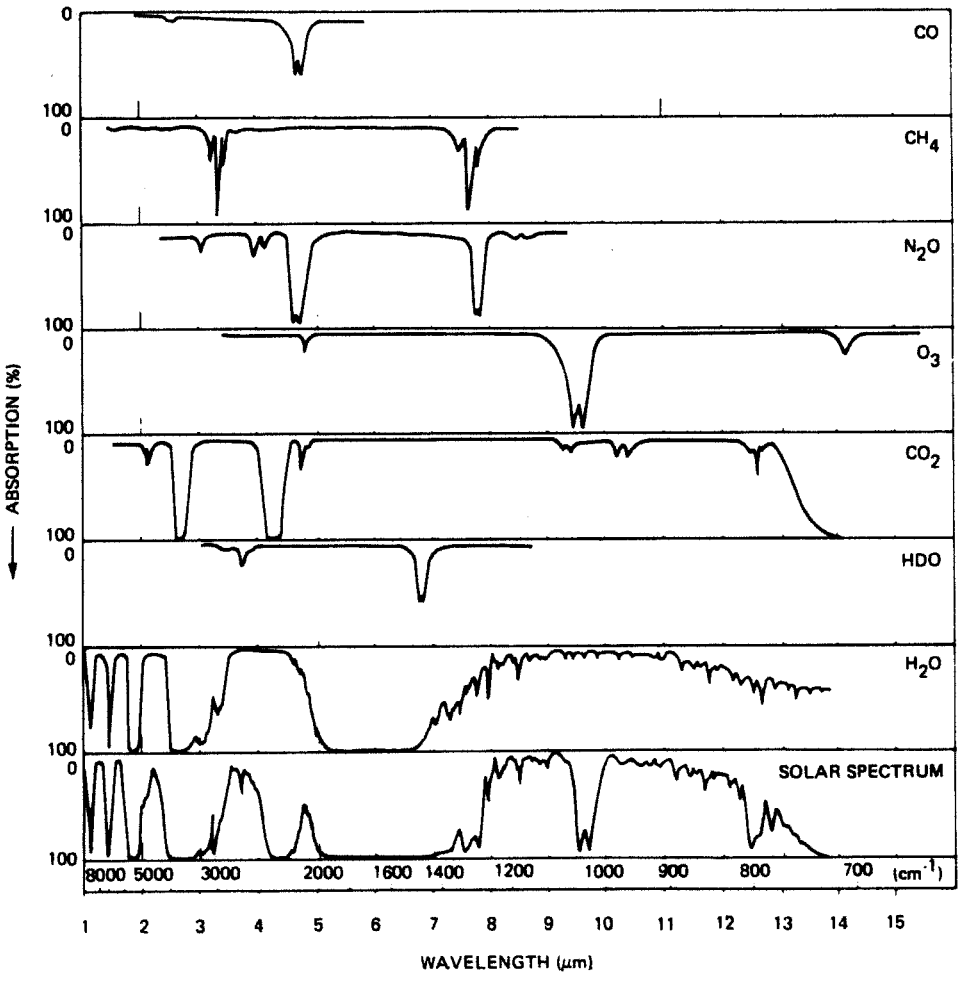

Figure 8-2. Absorption along a vertical atmosphere path by a variety of constituents in the spectral region from 1.0 to 16μm. (From J. H. Shaw, 1970.)

A number of models have been proposed to describe this distribution, and different ones are used to describe clouds, haze, or continental particulates.

Clouds completely obscure the surface in the visible and near-IR regions up to 3 μm because of scattering and, to some extent, absorption. At longer wavelengths, their effect is considerable up to the millimeter region; then they become gradually more transparent.

Cloud coverage varies considerably as a function of location and season. On the average, 40% of the Earth is cloud covered at any time. It is appreciably higher than this value in the tropical regions and appreciably lower over desert regions at midlatitude. In contrast, Venus is completely cloud covered all the time. The Venusian clouds are thought to consist of sulfuric acid droplets. They completely eliminate the use of visible or infrared sensors for imaging the surface. The same is true in the case of Titan, where a global layer of methane clouds/haze covers the surface and blocks its visibility in the visible and infrared regions.

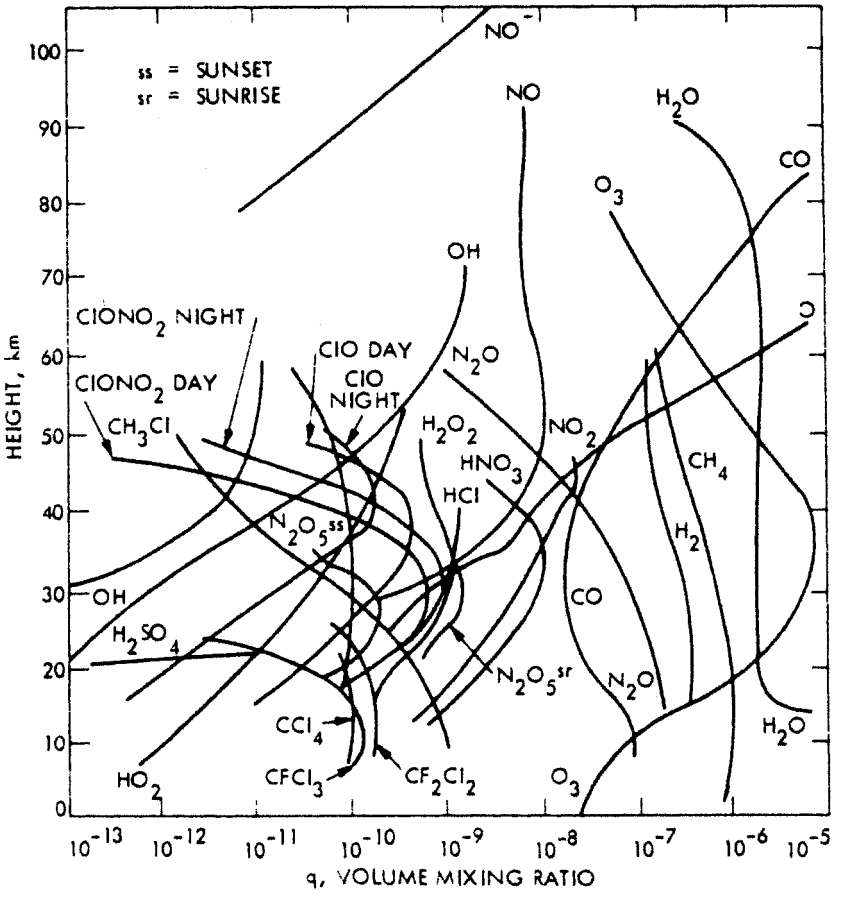

Figure 8-3. Distribution of some chemically active constituents in the Earth's atmosphere. (From Waters, 1984.)

8-4 WAVE INTERACTION MECHANISMS IN PLANETARY ATMOSPHERES

The interaction of electromagnetic waves with planetary atmospheres involves resonant interactions corresponding to molecular and atomic energy levels, nonresonant interactions, and refraction. In addition, suspended particles scatter the light waves and have their own radiative properties. These different interaction mechanisms are discussed in this section.

8-4-1 Resonant Interactions

When an electromagnetic wave interacts with a gaseous molecule, it may excite the molecule to a higher energy level and in the process transfer all or part of its energy to the molecule. A molecule in an excited state may drop to a state with a lower energy level and in the process emit energy in the form of an electromagnetic wave. The energy levels of gaseous molecules are well defined and discrete. Thus, the related interaction occurs at a

very specific frequency leading to spectral lines. The environmental factors, specifically temperature and pressure, lead to the broadening of these lines to narrow bands.

The basic mechanisms behind the energy states of gaseous molecules are similar to what was discussed in the case of solids (Chapters 2 and 3). Electronic energy levels result from the transfer of electrons between different orbits. Vibrational energy levels result from the different vibrational modes of the molecule. In addition, gaseous molecules have rotational energy states that correspond to rotation of the molecule around different axes. On the other hand, the interaction mechanisms that were related to the crystalline structure in solids, such as crystal field effects, semiconducting bands, and color centers, do not exist in the case of gases.

The lowest energy levels correspond to the rotational states. These levels depend on the three principal moments of inertia of the molecule. Four types of rotating molecules exist, some of which are shown in Figure 8-4:

1. All three principal moments of inertia are different. This is the case for H_2O. The molecule is called asymmetric top.
2. Two of the moments are equal. This is a symmetric top molecule.
3. All three moments are equal. This is the case for CH_4. The molecule is called spherical top.
4. Two of the moments are equal and the third one is negligible. This is the case of a linear molecule such as CO_2.

No energy transitions are allowed in the pure rotation spectrum for a molecule that possesses no permanent dipole moment. The symmetric linear CO_2 molecule is such an example.

To illustrate, let us consider the case of the water molecule and oxygen molecule; Figure 8-5 shows their rotational modes. The lowest spectral line for water vapor occurs at

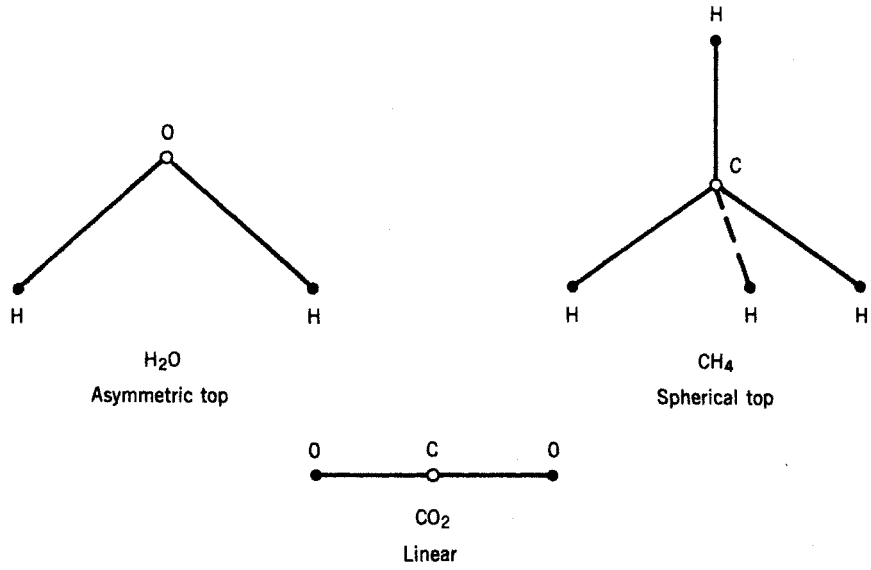

Figure 8-4. Three different molecules representing three different types of rotational effects.

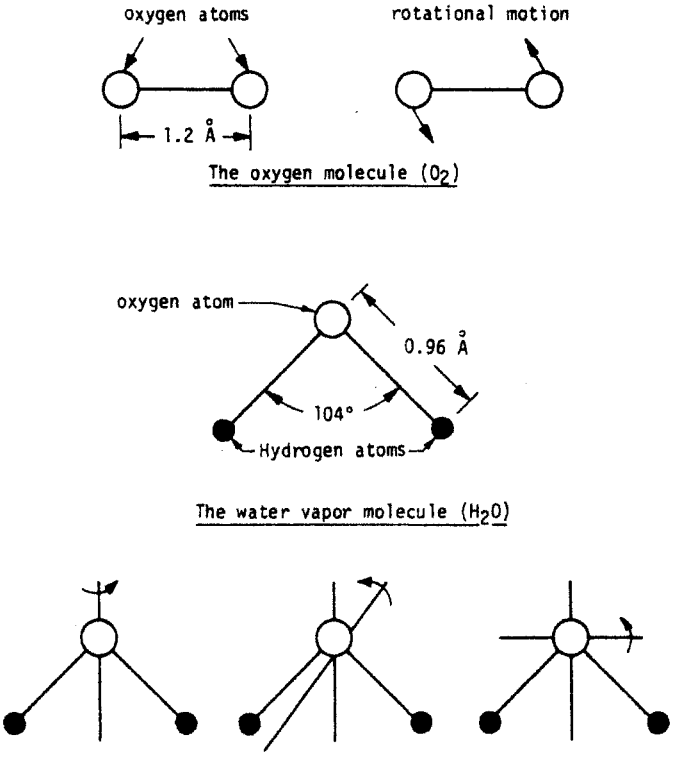

Figure 8-5. Rotational modes of the water and oxygen molecules.

22.2 GHz, the next-lowest one is at 183.3 GHz. Figure 8-6 shows the absorption spectrum of water vapor from 3 to 300 GHz at two pressure levels. An interesting observation is that as the pressure decreases, the absorption at the center of the line increases because the absorption from the same amount of water vapor is now limited to a narrower band.

The oxygen molecule has no permanent electrical dipole moment but has a permanent magnetic dipole moment resulting from the fact that two of the orbital electrons are unpaired. The two lowest spectral lines occur at 60 GHz (which is a band consisting of multiple lines) and 118.75 GHz (Fig. 8-7).

The absorption due to atmospheric oxygen and water vapor dominates the resonant interaction of waves in the Earth's lower atmosphere across the microwave spectrum from 20 GHz to 180 GHz.

In the upper atmosphere, the trace molecules play a more tangible role, and their spectral signature is usually very rich in spectral lines, as shown in Figure 8-8.

In the more simple model of a diatomic molecule and elementary calculation of the energy levels, the molecule can be regarded as a dumbbell consisting of two masses at a fixed distance. Let I be the moment of inertia relative to the axis perpendicular to the line connecting the two masses and intersecting it at the center of mass. In quantum mechanics, it can be shown that the corresponding rotational energy levels are given by

$$E = \frac{h}{8\pi^2 I} j(j+1) \tag{8-16}$$

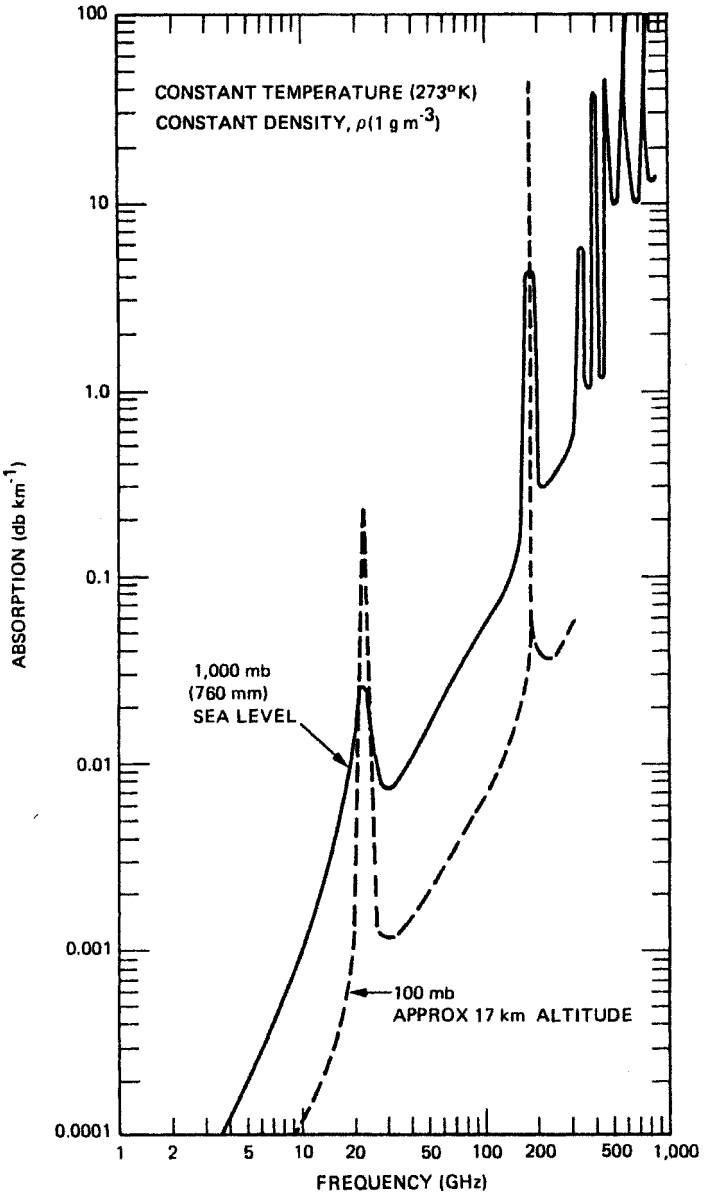

Figure 8-6. Absorption spectrum of water vapor at two pressures—1 bar and 0.1 bar—at temperature 273 K and for a water vapor density of 1 g/m^3 (from Chahine et al., 1983).

where j is the rotational quantum number ($j = 0, 1, 2, \ldots$). The selection rule requires that transitions can occur only between adjacent energy levels (i.e., $\Delta j = \pm 1$). Thus, the energy transfer for the transition from level j to $j - 1$ is

$$\Delta E_j = \frac{h}{8\pi^2 I}[j(j+1) - (j-1)j] = \frac{h}{4\pi^2 I} j \tag{8-17}$$

which indicates that the spectrum consists of a series of equidistant lines.

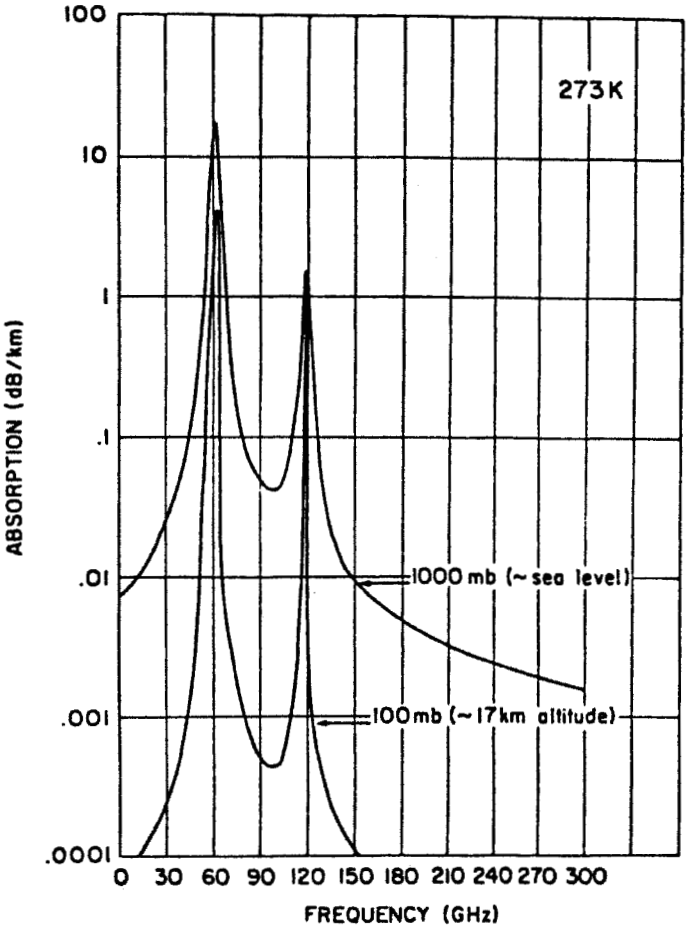

Figure 8-7. Absorption spectrum of atmospheric oxygen from 1 to 300 GHz for two pressures (1 bar and 0.1 bar) and at a constant temperature of 273 K (from Chahine et al., 1983).

The vibrational transitions correspond to significantly higher energy than the rotational transitions. Thus, the corresponding spectral lines appear mainly in the infrared region. One of the most important transitions used in atmospheric remote sensing is the 15 μm line of CO_2, which corresponds to the bending of the linear molecule.

As a molecule vibrates, its effective moment of inertia varies. Thus, we would expect the presence of a family of spectral lines around a vibrational line, which corresponds to rotation–vibration interactions. The rotational transitions appear as fine structure near the vibrational lines. This is clearly seen in the spectrum of the CO_2 molecule near the 15 μm band (wave number of 667 cm^{-1}).

The electronic transitions correspond to the highest energies, and the corresponding spectral lines are usually in the visible and ultraviolet part of the spectrum.

8-4-2 Spectral Line Shape

The spectral lines are not infinitely narrow. Line broadening results mainly from three factors: excited state lifetime, pressure-induced collisions, and thermal motion.

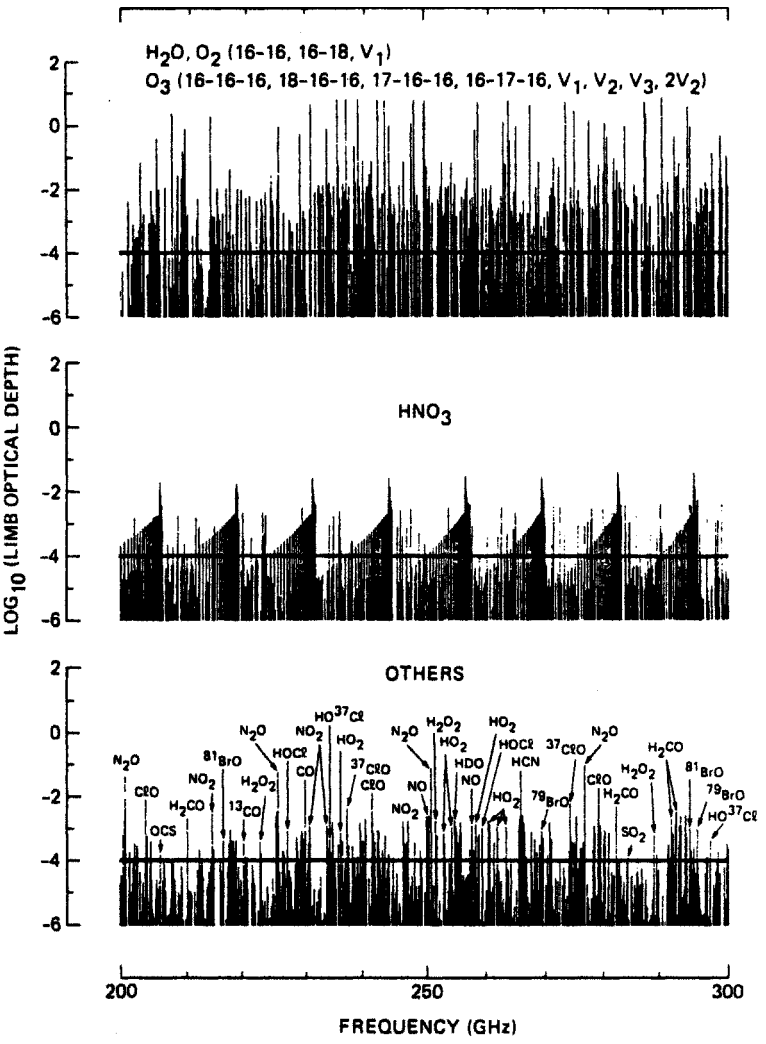

Figure 8-8. Spectral lines of a variety of atmospheric molecules in the Earth's upper atmosphere (from Waters et al., 1984).

If an excited state has a lifetime τ, the spectral line will have a frequency width Δv at least equal to:

$$\Delta v = \frac{1}{2\pi\tau} \tag{8-18}$$

This can be derived by assuming the emission from an excited state to be a pulse with exponentially decaying amplitude as a function of time. The Fourier transform of such a pulse will have a spectral width given by Equation 8-18.

The thermal motion of a molecule during emission or absorption of radiation gives rise to a Doppler shift. Considering that the thermal motion is random and the molecule's ve-

locity distribution is related to the temperature, it is normal to expect that the thermal motion induces a broadening of the spectral line. The resultant shape is given by

$$k(\nu) = \frac{S}{\nu_D\sqrt{\pi}} \exp\left[-\left(\frac{\nu - \nu_0}{\nu_D}\right)^2\right] \tag{8-19}$$

where S is a constant representing the total strength of the line [$S = \int_0^\infty k(\nu)d\nu$], ν_0 is the center frequency, and ν_D is the Doppler line width. ν_D is related to the gas temperature by

$$\nu_D = \frac{\nu_0}{c}\sqrt{\frac{2\pi RT}{M}} \tag{8-20}$$

where

R = universal gas constant = k/M_0 = 8314 JK^{-1} kg^{-1}
M = molecular weight of the gas
T = temperature of the gas

The Doppler broadening dominates at high altitudes.

Another mechanism of line broadening results from pressure-induced collisions. This is given by a Lorentz shape function:

$$k(\nu) = \frac{S}{\pi}\frac{\nu_L}{(\nu - \nu_0)^2 + \nu_L^2} \tag{8-21}$$

where ν_L is the Lorentz width. It is related to the mean time between collisions t_c by

$$\nu_L = \frac{1}{2\pi t_c} \tag{8-22}$$

The collision time in turn is inversely proportional to the pressure. Thus ν_L is linearly proportional to the pressure:

$$\frac{\nu_L}{P} = \frac{\nu_L(P_0)}{P_0} = \text{constant} \tag{8-23}$$

The Lorentz broadening dominates at high pressure and thus is particularly important at low altitudes. As shown in Figure 8-9*a*, the Lorentz broadening is slowly decaying and tends to have broad wings in comparison to Doppler broadening.

To illustrate the relative variation of the Doppler broadening and the pressure broadening, let us consider the lower 50 km of the Earth's atmosphere. In this layer, the pressure varies by three orders of magnitude, from 1 bar to 1 millibar, leading to a three orders of magnitude variation in the line broadening due to pressure. In comparison, the temperature varies by only 30%, between 300 K and 210 K. This leads to a change in the line broadening due to temperature of only about 14%. The drastic change in the pressure broadening of spectral lines allows the use of this effect for sounding of the atmospheric properties as a function of height.

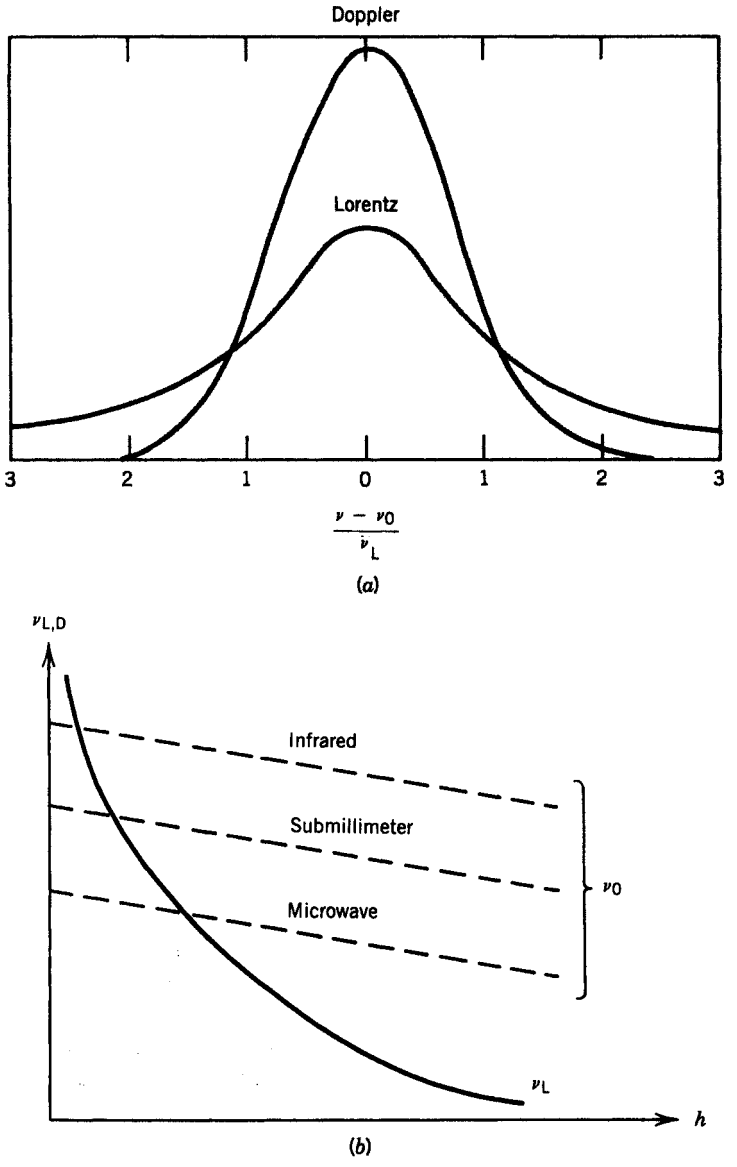

Figure 8-9. (*a*) Relative line shapes corresponding to Doppler broadening and Lorentz broadening. Both lines have the same strength and $\nu_L = \nu_D$. (*b*) The behavior of ν_L and ν_L as a function of altitude.

It should be noted that the Doppler broadening is proportional to ν_0. Thus, the Doppler effect will become particularly significant in the visible and infrared region of the spectrum (Fig. 8-9*b*).

8-4-3 Nonresonant Absorption

As seen in Figure 8-6, there is significant absorption that still occurs between spectral bands. The most common cause of absorption is a result of the slowly decaying wings of

distant spectral lines. The wings of the absorption lines, far away from the line center, fall off even slower than the Lorentz profile. However, the absorption does decrease significantly with pressure.

The two most-used atmospheric transparent windows in the infrared are at 3.5 μm to 4.1 μm and 10.5 μm to 12.5 μm. The latter one is particularly important because it is centered near the peak emission of a blackbody at typical Earth surface temperature. The main sources of absorption in the 11 μm window are the wings of the CO_2 lines at 15, 10.4, and 9.4 μm, and the wings of the neighboring water vapor lines. The effect of the CO_2 gas can be accurately modeled because it is uniformly mixed and has a relatively constant distribution. The water vapor contribution is hard to model because of its variability in space and time.

In the microwave region, continuous absorption is a result mainly of the water vapor (Fig. 8-6) and to a lesser extent oxygen (Fig. 8-7). It is clearly apparent that most of the absorption occurs in the lower atmosphere as a result of the high pressure and corresponding increase in the absorption coefficient.

In the case of Venus, the continuous absorption in the microwave region is mainly due to carbon dioxide and nitrogen (nitrogen absorption is also dominant for the Titan atmospheric), for which the absorption coefficient is given by (Ho et al., 1966)

$$\alpha_a = 2.610^7[f_{CO_2}^2 + 0.25 f_{CO_2} f_{N_2} + 0.005 f_{N_2}^2]\frac{v^2 P^2}{T^2} \tag{8-24}$$

where α_a is in km^{-1}, f is the volume mixing ratio, P is in atmosphere, v in GHz, and T in K. Figure 8-10 shows the total microwave absorption in the atmospheres of Venus and Titan.

If we consider a layer of gas of thickness dz and density ρ, the absorption through this layer is

$$\alpha_a \, dz = \rho\alpha \, dz \tag{8-25}$$

and the amount of intensity reduction encountered by an electromagnetic wave of intensity I is

$$dI = -\alpha_a \, dz \, I = -\rho\alpha \, dz \, I \tag{8-26}$$

α_a is called the absorption extinction coefficient, and α is called the absorption coefficient.

8-4-4 Nonresonant Emission

If we consider an atmospheric layer of thickness dz and temperature T, thermal radiation will be generated following Planck's law:

$$dI = \psi_t \, dz = \alpha_a B(v, T) dz \tag{8-27}$$

where $B(v, T)$ is the Planck function:

$$B(v, T) = \frac{2hv^3}{c^2} \frac{1}{\exp(hv/kT) - 1} \tag{8-28}$$

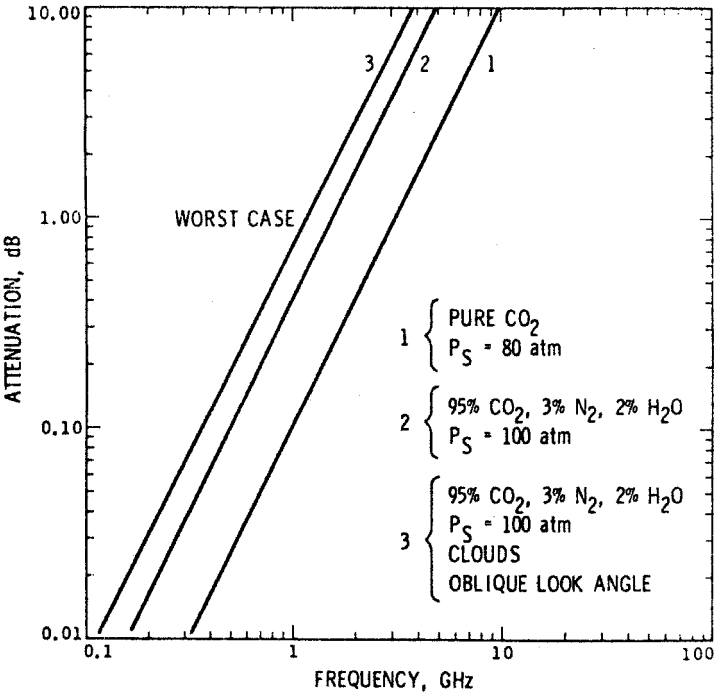

(*a*)

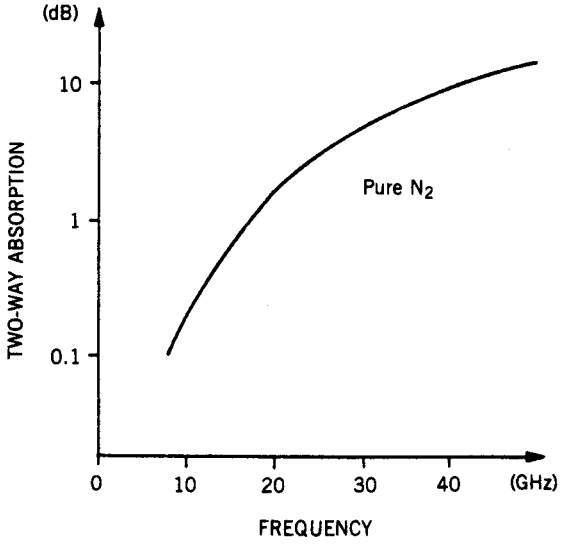

(*b*)

Figure 8-10. Total microwave absorption in the atmospheres of (*a*) Venus and (*b*) Titan over the frequency range from 1 to 30 GHz.

ψ_t is called the thermal source term. The reader should be careful when comparing the above equation to the expressions of the Planck function in Equations (2-30) and (4-1), where it is expressed as function of wavelength λ. The transformation is given by

$$B(v)dv = B(\lambda)d\lambda \Rightarrow B(v) = \frac{\lambda^2}{c}B(\lambda)$$

and the spectral radiance B is related to the spectral emittance S by

$$S = \pi B$$

In the case of planetary atmospheres, the temperature and constituent density are a function of the altitude z. Thus, the thermal source term is expressed as

$$\psi_t(z) = \alpha_a(z)B[v, T(z)] \tag{8-29}$$

8-4-5 Wave Particle Interaction and Scattering

In the most simple case, atmospheric particles can be considered as small spheres. The rigorous solution for the scattering of a plane monochromatic wave by a spherical dielectric particle with a complex index of refraction n was derived by Mie. The expressions for the scattering cross section and total extinction cross section are given by

$$\sigma_s = \frac{\lambda^2}{2\pi}\sum_{m=1}^{\infty}(2m+1)[|a_m(n,q)|^2 + |b_m(n,q)|^2] \tag{8-30}$$

$$\sigma_E = \frac{\lambda^2}{2\pi}\sum_{m=1}^{\infty}(2m+1)Re[a_m(n,q) + b_m(n,q)] \tag{8-31}$$

where the coefficients a_m and b_m are coefficients in the scattered field representing contributions from the induced magnetic and electric dipoles, quadrupoles, and so on. These coefficients can be expressed in terms of spherical Bessel functions with arguments $q = \pi D/\lambda$. D is the diameter of the sphere.

In the case of a small particle relative to the wavelength ($q \gg 1$), the above scattering cross sections reduce to

$$\sigma_s = \frac{2}{3}\frac{\pi^5 D^6}{\lambda^4}|K|^2 \tag{8-32}$$

$$\sigma_E = \frac{\pi^2 D^3}{\lambda} Im(-K) + \frac{2}{3}\frac{\pi^5 D^6}{\lambda^4}|K|^2 \tag{8-33}$$

where $K = (n^2 - 1)/(n^2 + 2)$. The absorption cross section σ_a is given by

$$\sigma_a = \sigma_E - \sigma_s \tag{8-34}$$

If the atmospheric unit volume contains N particles of equal size, the medium is then characterized by a particle extinction coefficient α_E given by:

$$\alpha_E = \sigma_E N \tag{8-35}$$

If the scattering particles have a size distribution given by , then

$$\alpha_E = \int \sigma_E(r) N'(r) dr \tag{8-36}$$

Similar expressions can be written for the scattering coefficient α_s and the absorption coefficient α_a. In the above expressions, multiple scattering has been neglected.

When the wave scatters from a particle, the scattered intensity has an angular pattern called the phase function $p(\theta_i, \theta_s, \phi_i, \phi_s)$ where θ_i and ϕ_i are the angles of the incident wave and θ_s and ϕ_s are the angles of the scattered wave. In simple terms, the phase function can be thought of as (1) the percentage of energy scattered per unit solid angle in a certain direction, (2) an angular weighting function for the scattered radiation, or (3) the equivalent of an antenna radiation pattern.

8-4-6 Wave Refraction

As a wave propagates in a medium, its speed differs from the wave speed in vacuum due to interaction with the medium constituents. This is characterized by the medium index of refraction n, which equals the ratio of the wave speed in vacuum to the wave speed in the medium. Thus, n is always greater than unity.

In the case of a gas mixture of oxygen, water vapor, and carbon dioxide similar to the Earth's atmosphere, the index of refraction for frequencies less than 200 GHz is given by

$$N = (n - 1)\, 10^6 = 0.0776 \frac{P}{T} + 373 \frac{e}{T^2} \tag{8-37}$$

where e is the partial pressure of water vapor in bar, P is the total pressure in bar, and N is called the refractivity. Under mean conditions, P, e, and T decrease with height such that N decreases roughly exponentially with height. Thus, the atmosphere can be considered as a spherically inhomogeneous shell. A wave incident obliquely on the top of the atmosphere will refract and therefore has a curved trajectory as it propagates through the atmosphere. This effect is used in occultation experiments to derive information about planetary atmospheres.

8-5 OPTICAL THICKNESS

Let us consider an atmospheric thin slab of thickness D. An incident monochromatic wave will be partially scattered and absorbed as it propagates through the slab. If α is the total extinction coefficient (including absorption and scattering), the intensity loss is

$$dI = -\alpha I\, dz \Rightarrow I(z) = I_0 e^{-\alpha z} \tag{8-38}$$

At the output of the slab the intensity is

$$I(D) = I_0 e^{-\alpha D} \tag{8-39}$$

The slab is thus characterized by a transmission coefficient,

$$T = e^{-\alpha D} \tag{8-40}$$

The term αD is usually called the slab optical thickness τ. If the slab is inhomogeneous (i.e., α varies with altitude z) and covers the altitudes from z_1 to z_2, then the slab optical thickness is

$$\tau(\nu, z_1, z_2) = \int_{z_1}^{z_2} \alpha(\nu, z) dz \tag{8-41}$$

and the slab transmission coefficient is given by

$$T(\nu) = e^{-\tau} \tag{8-42}$$

The total normal optical thickness of a planet's atmosphere is given by

$$\tau(\nu) = \int_0^{\infty} \alpha(\nu, z) dz \tag{8-43}$$

The optical thickness at an altitude z is defined as

$$\tau(\nu, z) = \int_z^{\infty} \alpha(\nu, \zeta) d\zeta \tag{8-44}$$

In the case where the wave is oblique, at an incidence angle θ, then

$$\tau(\theta, \nu, z) = \frac{\tau(\nu, z)}{\cos \theta} \tag{8-45}$$

If the extinction coefficient α decreases exponentially with altitude,

$$\alpha(\nu, z) = \alpha(\nu, 0) \exp \frac{-z}{H} \tag{8-46}$$

the optical thickness is then

$$\tau(\nu, z) = \int_z^{\infty} \alpha(\nu, 0) \exp \frac{-\zeta}{H} d\zeta = H\alpha(\nu, 0) \exp \frac{-z}{H} \tag{8-47}$$

and

$$\tau(\nu, 0) = H\alpha(\nu, 0) \tag{8-48}$$

If an atmosphere consists of a mixture of gases and particles, the total optical thickness is equal to the sum of the individual optical thicknesses:

$$\tau = \sum_g \tau_g + \sum_p \tau_p \tag{8-49}$$

The "optical thickness" is a parameter that is very widely used to characterize atmospheres.

8-6 RADIATIVE TRANSFER EQUATION

The radiative transfer equation is the fundamental equation describing the propagation of electromagnetic radiation in a scattering and absorbing medium. At a given point in the medium, the change in the intensity $I(z, \theta, \phi)$ as the wave traverses a distance dz in the direction (θ, ϕ) consists of the following elements (see Fig. 8-11).

The wave is attenuated due to absorption in the gas and the suspended particles. This corresponds to change of the wave energy to heat. The corresponding intensity loss is given by

$$\frac{dI}{dz} = -\alpha_a I \tag{8-50}$$

where α_a is the sum of the absorption coefficient of all the gases and particles in the medium.

Some of the wave energy is scattered by the particles, which results in a loss of intensity in the (θ, ϕ) direction, even though the total wave energy is conserved. The corresponding intensity loss is given by

$$\frac{dI}{dz} = -\alpha_s I \tag{8-51}$$

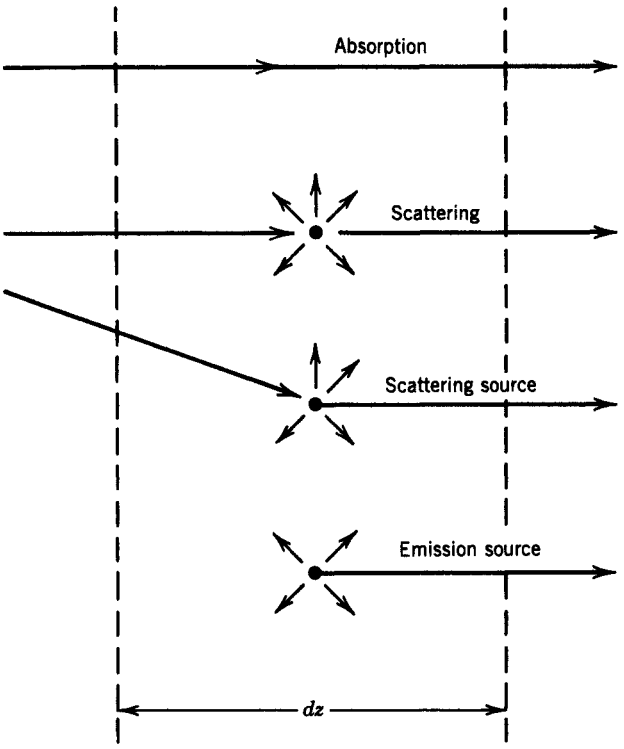

Figure 8-11. The different elements that contribute to the radiation transfer equation.

Some energy is added to the wave as a result of thermal emission from the medium. This source term is given by

$$\frac{dI}{dz} = \psi_t(z) = +\alpha_a B(\nu, T) \tag{8-52}$$

Some energy is added to the wave in the (θ, ϕ) direction as a result of scattering of waves incident from other directions. This source term is given by

$$\frac{dI}{dz} = \psi_s = \alpha_s(z) J(\theta, \phi) \tag{8-53}$$

where

$$J(\theta, \phi) = \frac{1}{4\pi} \int_0^{4\pi} I(\theta', \phi') p(\theta', \theta, \phi', \phi) d\Omega'$$

In the above expression, p is the scattering phase function that describes the angular distribution of the scattered field. Therefore, the radiative transfer equation can be written as

$$\frac{dI}{dz} = -\alpha_a I - \alpha_s I + \alpha_a B + \alpha_s J \tag{8-54}$$

or, in a more simplified form,

$$\frac{dI}{dz} = -\alpha(z) I + \psi(z, \theta, \phi) \tag{8-55}$$

where the loss terms and the source terms are combined.

The radiative equation is often written using the medium elementary optical thickness $d\tau = -\alpha\, dz$ as a variable. From Equation 8-54 we can write

$$\frac{dI}{d\tau} = +I - \frac{\alpha_a}{\alpha} B - \frac{\alpha_s}{\alpha} J \tag{8-56}$$

or

$$\frac{dI}{d\tau} = +I - (1 - \omega) B - \omega J \tag{8-57}$$

where

$$\omega = \frac{\alpha_s}{\alpha}$$

The solution of the radiative transfer equation is very involved in the general case, and usually simplifying assumptions and numerical methods are used. The reader is referred to the book by Chandrasekhar, *Radiative Transfer,* for a good study of the solution methods.

The radiative equation solutions become even more involved when the polarization of the wave is also included. In this case, three additional parameters have to be accounted for in addition to the wave intensity. These are degree of polarization, polarization plane, and ellipticity.

Most of the techniques used in practical remote sensing situations use numerical methods. One such technique is the Monte Carlo technique, in which photons are followed through the atmosphere as they get absorbed and scattered in a probabilistic sense. This method can be used with homogeneous as well as inhomogeneous atmospheres.

8-7 CASE OF A NONSCATTERING PLANE PARALLEL ATMOSPHERE

To illustrate, let us consider the case of a nonscattering atmosphere in which the geometry is plane parallel (see Fig. 8-12). Let us consider the case of a wave propagating at an angle θ relative to the vertical. We assume that the semiinfinite atmosphere is bounded at $z = 0$, which is also the origin for the optical thickness variable ($\tau = 0$). The radiative transfer equation can be written as

$$\cos\theta \frac{dI}{d\tau} = I(\tau, 0) - B$$

or

$$\mu \frac{dI}{d\tau} = I(\tau, \mu) - \psi(\tau, \mu) \tag{8-58}$$

where $\mu = \cos\theta$ and ψ is the source term ($\psi = \psi_\tau/\alpha_a$). The solution of the above equation is given by

$$I(\tau, \mu) = Ae^{\tau/\mu} + \frac{1}{\mu}\int_{\tau}^{\tau_0} \psi(\eta, \mu) e^{(\tau-\eta)/\mu}\, d\eta \tag{8-59}$$

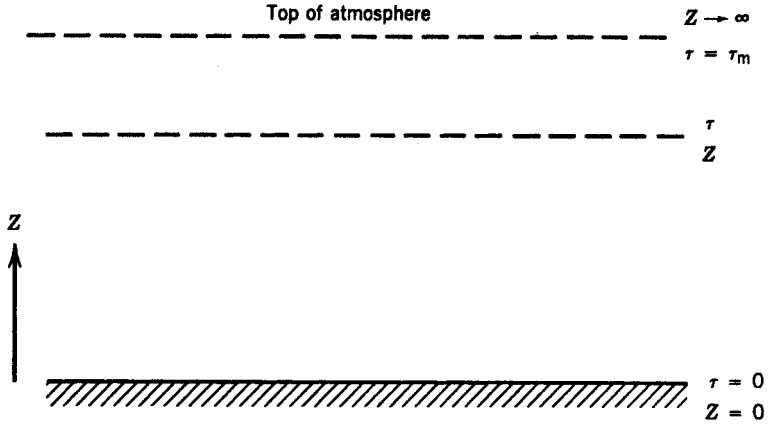

Figure 8-12. Geometry for the case of a plane parallel atmosphere.

where A and τ_0 are constants. τ varies from $\tau = 0$ to $\tau = \tau_m$, where τ_m is the optical thickness of the total atmospheric layer.

In the case of inward radiation from the atmosphere toward the surface, the total intensity at level τ is

$$I(\tau, \mu) = \frac{1}{\mu}\int_{\tau}^{\infty} \psi(\eta, \mu) e^{(\tau-\eta)/\mu}\, d\eta \tag{8-60}$$

In the case of outward radiation toward space,

$$I(\tau, -\mu) = I(0, -\mu)e^{-\tau/\mu} + \frac{1}{\mu}\int_{0}^{\tau} \psi(\eta, -\mu) e^{-(\tau-\eta)/\mu}\, d\eta \tag{8-61}$$

and if the observing point is above the atmosphere, then

$$I(\tau_m, -\mu) = I(0, -\mu)e^{-\tau m/\mu} + \frac{1}{\mu}\int_{0}^{\tau_m} \psi(\eta, -\mu) e^{-(\tau-\eta)/\mu}\, d\mu \tag{8-62}$$

where $I(0, -\mu)$ is the intensity of the upward radiation in the direction μ at the surface, and τ_m is the total optical thickness of the atmosphere.

8-8 BASIC CONCEPTS OF ATMOSPHERIC REMOTE SOUNDING

The techniques of atmospheric sounding can be divided into three general categories: occultation, scattering, and emission.

In the case of occultation techniques, the approach is to measure the changes that the atmosphere imparts on a signal of known characteristics as this signal propagates through a portion of the atmosphere. The signal source can be the sun, a star, or a man-made source such as a radio or radar transmitter. The geometry corresponds usually to limb sounding. Figure 8-13*a* shows the case in which the sun is used as a source, whereas Figure 8-13*b* shows the case in which a spacecraft radio transmitter is the source. This latter case is commonly used in planetary occultation. A special configuration is shown in Figure 8-13*c* in which the surface is used as a mirror to allow the signal to pass through the total atmosphere twice.

In the case of scattering, the approach is to measure the characteristics of the scattered waves in a direction or directions away from the incident wave direction. The source can be the sun, as in Figure 8-13*d*, or man-made, as in Figure 8-13*e*.

In the case of emission, the radiation source is the atmosphere itself (Figs. 8-13*f* and *g*), and the sensor measures the spectral characteristics and intensity of the emitted radiation.

The different atmospheric sounding techniques aim at measuring the spatial and temporal variations of the atmospheric properties, specifically temperature profile, constituents nature and concentration, pressure, wind, and density profile. In the rest of this section, the techniques used for measuring these properties are briefly described in order to give an overview of the following three chapters.

8-8-1 Basic Concept of Temperature Sounding

If a sensor measures the radiation emitted from gases whose distribution is well known, such as carbon dioxide or molecular oxygen in the Earth's atmosphere, then the radiance

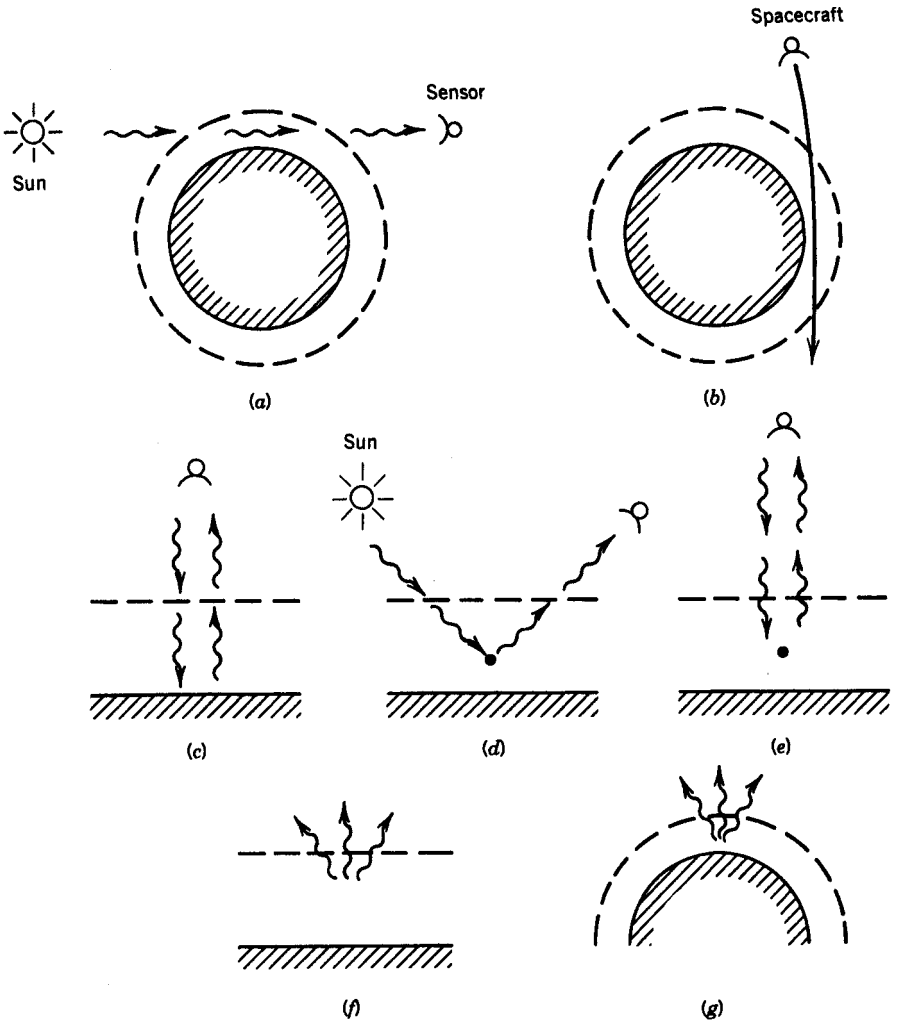

Figure 8-13. Different configurations for atmospheric sounding (see text for explanation).

can be used to derive the temperature (Equation 8-29). At first glance, it seems that only the mean temperature can be derived because the radiation detected at any instant of time is a composite of waves emitted from all the different layers in the atmosphere. However, if we can measure the radiance variation as a function of frequency near a spectral line, the temperature vertical profile can be derived. This can be explained as follows.

The contribution from the layers at the top of the atmosphere is very small because the density (i.e., number of radiating molecules) is low. As we go deeper in the atmosphere, the contribution increases because of the higher atmospheric density. However, for the deep layers near the surface, even though the radiation source is the largest, the emitted radiation has to traverse the whole atmosphere, where it gets absorbed. Thus, its net contribution to the total radiance is small. This implies that, for a certain atmospheric optical thickness, there is an optimum altitude layer for which the combination of gas density

(i.e., source strength) and attenuation above it are such that this layer contributes most to the total radiance. If the optical thickness changes, then the altitude of the peak contribution changes. Thus, if we observe the radiance at a number of neighboring frequencies for which the optical thickness varies over a wide range (this occurs when we look around an absorption spectral band), the altitude of the contribution peak will vary, thus allowing temperature measurement at different altitudes. This technique will be formulated quantitatively and discussed in detail in Chapter 9.

In order to get an accurate temperature profile, the absorption band used should have the following properties:

1. The emitting constituent should have a known mixing ratio and preferably be uniformly mixed in the atmosphere. This is the case for molecular oxygen and carbon dioxide in the Earth's atmosphere up to 100 km. The most commonly used bands are the 60 GHz band for oxygen and the 15 μm and 3.4 μm infrared bands for carbon dioxide. In the case of the Martian and Venusian atmospheres, CO_2 infrared bands can be used. In the case of Jupiter, methane is uniformly mixed and its 7.7 μm infrared line can be used.
2. The absorption band involved should not be overlapped by bands from other atmospheric constituents. The 60 GHz oxygen line in the Earth's atmosphere, the 15 μm CO_2 line in the Earth, Mars, and Venus atmospheres, and the 7.7 μm CH_4 line in the Jovian atmosphere satisfy this requirement.
3. Local thermodynamic equilibrium should apply so that the Planck emission law is appropriate. This is usually the case in the lower 80 km of the Earth's atmosphere.
4. The wavelength should be long enough such that the scattered solar radiation is insignificant compared to the thermal emission. This is always the case in the microwave, millimeter, and thermal infrared part of the spectrum.

8-8-2 Basic Concept of Composition Sounding

The identification of atmospheric constituents is usually based on detecting the presence of a spectral line or lines associated with a certain molecule. The spectral signature is in effect the "fingerprint" of a gaseous constituent.

In order to determine the abundance of a constituent, a more detailed analysis of the spectral signature is required. The line strength is usually related to the number density of molecules. This usually requires knowledge of the local pressure and temperature. Once the temperature is derived using the radiance from a homogeneously mixed constituent as discussed earlier, the corresponding abundance profiles can be derived by measuring the spectral radiance around other spectral lines. The "sounding" spectral lines should satisfy the same properties discussed in the previous section except for the first one, which is relevant only to temperature sounding.

8-8-3 Basic Concept of Pressure Sounding

The total columnar absorption is strongly related to the columnar mass of a constituent in the atmosphere, particularly near a resonant line of the constituent. If the constituent is homogeneously mixed in the atmosphere, its total mass is then directly proportional to the surface pressure. Thus, surface pressure sounding can be achieved by devising a tech-

nique to measure the total columnar absorption of a homogeneously mixed gas such as oxygen in the Earth's atmosphere.

8-8-4 Basic Concept of Density Measurement

The atmospheric refractivity N is directly proportional to the atmospheric density. Thus, one approach is to derive the refractivity profile as a function of altitude. This is done to derive the density profile of planetary atmospheres using the refraction of the radio communication signal as orbiting or flyby spacecraft are occulted by the atmosphere. The radio occultation technique is discussed in more detail in Chapter 9.

8-8-5 Basic Concept of Wind Measurement

The simplest technique for wind measurement is to take a time series of cloud photographs, which would allow derivation of the wind field at cloud level. In order to get the wind field at any other altitude, the Doppler effect is used. The Multi-angle Imaging SpectroRadiometer (MISR) instrument that flies on the Terra spacecraft uses a series of images taken forward and aft of the spacecraft at different look angles and image matching algorithms to measure vector winds at the cloud levels.

Any molecule in motion will have its spectral line shifted by the Doppler effect. The Doppler shift is equal to

$$\Delta v = \frac{V}{\lambda} \cos \theta$$

where λ is the line wavelength and $V \cos \theta$ is the molecule velocity along the line of observation. Thus, by accurately measuring the line center for a known atmospheric constituent and comparing it to the frequency of the line for the same constituent in a static case, one of the velocity components can be derived. To illustrate, if a carbon dioxide molecule is moving at a line of sight velocity of 1 m/sec, the 15 μm line will have a frequency shift of

$$\Delta v = \frac{1}{15 \times 10^{-6}} \simeq 66.7 \text{ kHz}$$

which is small but measurable. If we use the oxygen line at 60 GHz, then

$$\Delta v = \frac{1}{5 \times 10^{-3}} = 200 \text{ Hz}$$

Another technique for wind measurement, also based on the Doppler effect, uses the scattered wave from an illuminating laser or radar beam. The incident wave is scattered by moving particles and the returned signal is shifted by a frequency Δv given by

$$\Delta v = \frac{2V}{\lambda} \cos \theta$$

The returned signal is then mixed with a reference identical to the transmitted signal to derive the Doppler shift.

EXERCISES

8.1. A planetary atmosphere is composed of two gases, G_1 and G_2. The molecular weight of gas G_2 is half that of gas G_1. At a height of 10 km, the number densities of the two gases were measured to be equal. Assuming that the scale height of gas G_1 is 15 km and that the temperature is constant in altitude, then:

(a) Calculate the scale height of gas G_2.

(b) Calculate the ratio of number densities of gas G_1 to G_2 at the surface.

(c) Calculate the ratio at altitude of 30 km.

(d) Calculate the ratio of the total number of atoms of gas G_1 above 30 km to the total number of atoms of gas G_2 above 30 km.

(e) Calculate the ratio of the total mass of the two gases.

(f) Calculate the altitude at which the total mass is 1% of the mass at the surface.

8.2. A planetary atmosphere is characterized by a scale height H and a surface number density $N(0)$. A photon flux F_0 at a certain wavelength strikes the top of the atmosphere. If σ is the absorption cross section in square meters of the atmospheric gas, calculate:

(a) The flux at altitudes $2H$, H, $H/2$, and the surface.

(b) The ratio of the flux at a certain height h to the flux at height $h + H$.

8.3. Let us assume that the scale height is a linear function of altitude:

$$H = H_0 + ah$$

where H_0 and a are constants. Give the expression of the number density and the pressure as a function of altitude. Compare the two cases in which $H_0 = 10$ km, $a = 0.5$, and $H_0 = 1$ km, $a = 0$

8.4. Derive the analytical expression, then calculate the ratio of σ_s/σ_a over the wavelength region $0.1\ \mu\text{m} \leq \lambda \leq 10\ \mu\text{m}$ for the case of particles characterized by the following radius and index of refraction:

(a) $r = 0.5\ \mu$m, $n = 1.5 + i0.001$

(b) $r = 0.5\ \mu$m, $n = 1.5 + i0.01$

(c) $r = 2.0\ \mu$m, $n = 1.5 + i0.001$

(d) $r = 2.0\ \mu$m, $n = 1.5 + i0.01$

Assume that the imaginary part of the index of refraction is much smaller than the real part.

8.5. Repeat the previous exercise for the wavelength region $1\ \text{cm} \leq \lambda \leq 10$ cm and for

(a) $r = 1$ mm, $n = 7 + i1$

(b) $r = 1$ mm, $n = 2 + i0.01$

8.6. Using Equations (8-19) and (8-21) for the Doppler and Lorentz line-shape broadening, calculate the pressure in the atmosphere at which the half amplitude width due to collision broadening is equal to that due to Doppler broadening for the following spectral lines:

(a) Carbon dioxide line at 15 μm

(b) Water vapor line at 6.25 μm

(c) Water vapor line at 0.1 mm

Assume that all lines have collision-broadening half width of $\Delta\nu = 3$ GHz at the surface pressure of 1 bar. Also, assume that $M = 29$ and $T = 273$ K.

REFERENCES AND FURTHER READING

Caulson, K., J. Dave, and Z. Sekera. *Tables Related to Radiation Emerging from a Planetary Atmosphere with Rayleigh Scattering.* University of California Press, Los Angeles, 1960.

Chahine, M. T., et al. Interaction mechanisms within the atmosphere. In *Manual of Remote Sensing.* American Society of Photogrammetry, Falls Church, VA, 1983.

Chandrasekhar, S. *Radiative Transfer.* Oxford University Press, 1950.

Chen, M., R. B. Rood, and W. G. Read. Seasonal variations of upper tropospheric water vapor and high clouds observed from satellites. *Journal of Geophysics Research,* **104,** 6193–6197, 1999.

Dessler, A. E., M. D. Burrage, J.-U. Grooss, J. R. Holton, J. L. Lean, S. T. Massie, M. R. Schoeberl, A. R. Douglass, and C. H. Jackman. Selected science highlights from the first 5 years of the Upper Atmosphere Research Satellite (UARS) program. *Review of Geophysics,* **36,** 183–210, 1998.

Diner, D. J., J. C. Beckert, T. H. Reilly, C. J. Bruegge, J. E. Conel, R. Kahn, J. V. Martonchik, T. P. Ackerman, R. Davies, S. A. W. Gerstl, H. R. Gordon, J-P. Muller, R. Myneni, R. J. Sellers, B. Pinty, and M. M. Verstraete. Multi-angle Imaging SpectroRadiometer (MISR) description and experiment overview. *IEEE Transactions on Geoscience and Remote Sensing,* **36,** 1072–1087, 1998.

Drouin, B. J., J. Fisher, and R. R. Gamache. Temperature dependent pressure induced lineshape of O_3 rotational transitions in air. *Journal of Quantitative Spectroscopy and Radiative Transfer,* **83,** 63–81, 2004.

Hansen, J. E., and L. D. Travis. *Space Science Review,* **16,** 527, 1974.

Herman, B. M., S. R. Bowning, and R. J. Curran. The effects of atmospheric aerosols on scattered sunlight. *Journal of Atmospheric Science,* **28,** 419–428, 1971.

Ho, W., et al. Laboratory measurements of microwave absorption in models of the atmosphere of Venus. *Journal of Geophysics Research,* **21,** 5091–5108, 1966.

Liou, K. N. *An Introduction to Atmospheric Radiation* (2nd ed.). Academic Press, San Diego, 2002.

Oh J. J., and E. A. Cohen. Pressure broadening of ozone lines near 184 and 206 GHz by nitrogen and oxygen. *Journal of Quantitative Spectroscopy and Radiative Transfer,* **48,** 405–408, 1992.

Pickett, H. M., D. E. Brinza and E. A. Cohen. Pressure broadening of ClO by nitrogen. *Journal of Geophysics Research,* **86,** 7279–7282, 1981.

Rodgers, C. D. *Inverse Methods for Atmospheric Sounding: Theory and Practice.* World Scientific Publishing Co. Ltd., Singapore, 2000.

Shaw, J. H. Determination of the Earth's surface temperature from remote spectral radiance observation near 2600 cm^{-1}. *Journal of Atmospheric Science,* **27,** 950, 1970.

Thomas, G. E., and K. Stamnes. *Radiative Transfer in the Atmosphere and Ocean.* Cambridge University Press, Cambridge, 1999.

Van de Hulst, H. C. *Light Scattering by Small Particles.* Wiley, New York, 1957.

Waters, J., et al. A balloon borne microwave limb sounder for stratospheric measurements. *Journal of Quantitative Spectroscopy and Radiative Transfer,* **32,** 407–433, 1984.

Waters, J. W., et al. The UARS and EOS Microwave Limb Sounder Experiments. *Journal of Atmospheric Science,* **56,** 194–218, 1999.